Heliyon 10 (2024) e34666

Contents lists available at ScienceDirect

Heliyon

journal homepage: www.cell.com/heliyon

Research article

DFT study on the depolymerization of PET by Ca-catalyzed glycolysis reaction model

Anyarin Arunphacharawit [a], Thinnaphat Poonsawat [a], Titiya Meechai [b], Laksamee Chaicharoenwimolkul Chuaitammakit [c], Ekasith Somsook [a,*]

[a] *NANOCAST Laboratory, Center for Catalysis Science and Technology (CAST), Department of Chemistry and Center of Excellence for Innovation in Chemistry, Faculty of Science, Mahidol University, 272 Rama VI Road., Ratchathewi, Bangkok, 10400, Thailand*
[b] *Department of Premedical Science, Faculty of Medicine, Bangkokthonburi University, Thawi Watthana, Bangkok, 10170, Thailand*
[c] *Chemistry and Applied Chemistry, Faculty of Science and Technology, Suratthani Rajabhat University, 272 Moo 9, Surat-Nasan Road, Khuntale, Muang, Surat Thani, 84100, Thailand*

ARTICLE INFO

Keywords:
Chemical recycling
Poly(ethylene terephthalate)
Poly(ethylene furanoate)
DFT calculation
Conformational structure
Calcium catalyst

ABSTRACT

Poly(ethylene terephthalate) (PET) is the most common plastics produced for applications in food and drinking containers. It is degraded to valuable product by several methods. Glycolysis of PET gains *bis*(2-hydroxyethylene) terephthalate (BHET) as the main product utilized as plasticizer. Calcium catalysts, Ca^{2+} and $Ca(OH)_2 \bullet 2H_2O$ were explored to study the mechanism of PET cleavage by DFT calculations at B3LYP/6-311++G** level. Two possible pathways, coordination, and non-coordination of ethylene glycol on the calcium in glycolysis reaction, have been investigated. In addition, poly(ethylene furanoate) (PEF), considered as a sustainable polymer with the similar functional properties, was chose for the comparison of conformational structures with PET. The understanding of the relationship between PET (and PEF) structures and calcium catalysts is useful for the future development of linear sustainable polyesters.

1. Introduction

The transportation of microplastics *via* the food chain is a concerning ecological phenomenon. These tiny plastic particles infiltrate oceans, ingested by small organisms, accumulating as they transfer in the food chain. From plankton to humans consuming seafood, the impact is far-reaching, posing threats to marine life and potential health risks for humans [1,2]. Addressing this issue requires immediate action to mitigate plastic pollution, improve waste management, and protect our ecosystems from the pervasive presence of microplastics.

Poly(ethylene terephthalate) (PET) is a common thermoplastic in the polyester family with excellent combination properties for several applications [3,4]. The applications of PET were utilized in food and drinking containers. However, most of PET in markets are used as drinking bottles for pure water, soft drink, and alcohol beverages which post-consumer drinking bottles are left as waste in many places [5–7]. The mismanagement of plastics has become an important issue that is crucial in many countries which can be observed by the policy for the reduction of the uses and recycling of plastics.

There are many chemical recycling methods proposed for depolymerization of PET [8–12] such as hydrolysis, methanolysis, ammonolysis, aminolysis, and glycolysis as shown in Fig. 1. Glycolysis is the most important method that is widely used on a

* Corresponding author.
E-mail address: ekasith.som@mahidol.ac.th (E. Somsook).

https://doi.org/10.1016/j.heliyon.2024.e34666
Received 24 January 2024; Received in revised form 28 June 2024; Accepted 15 July 2024
Available online 17 July 2024

commercial scale for the depolymerization of PET proceeded by using transesterification reaction. The broader range of temperature was studied in glycolysis reaction (180-300 °C). The valuable *bis*(2-hydroxyethylene) terephthalate (BHET) product that can be re-inserted in the production line of PET and can be used in textile softeners and unsaturated poly ester-resin. It drives the glycolysis become the most interesting process in the chemical recycling of PET [13]. Glycolysis of PET without catalysts required the extreme condition (supercritical glycolysis) resulting in worthless and non-eco-friendly processes. The popular improvement of increasing reaction rate was presented in the scope of catalysts [14]. One of the various catalysts commonly used in PET glycolysis is zinc acetate, as the activation of reaction by this catalyst is remarkable [15]. Other metal salts (MX), such as acetate (M = Co, Pb, and Mn) [16], chloride (M = Zn, Li, Fe, and Didymium) [17], hydroxide (M = Li, K) [18,19], sulphate (M = Na, K) [18], titanium phosphate [20], and sodium carbonate [21,22], have been investigated. Recently, ionic liquids have been processed for the glycolysis reaction of PET. However, the ionic liquid catalyst is impractical in the synthetic process [23], high toxicity and erosivity [24–27], lower percentage in PET conversion and BHET selectivity compared to metal oxide as a catalyst [28–32]. Many efforts have been made by researchers to find affordable catalysts and reaction systems [33].

Various heterogeneous metal oxide catalysts have been tested in PET glycolysis [33–35]. In our research group, we reported the use of calcium oxide catalysts derived from natural and industrial byproducts for the glycolysis of post-consumer PET drinking bottles. The catalyst precursors can be obtained from ostrich eggshells, chicken eggshells, oyster shells, geloina shells, and mussel shells at local markets. This promising catalyst could reach 75 % yield of BHET from the glycolysis of PET. The result was interestingly higher than the control experiment using commercial zinc acetate catalyst. These findings suggest that calcium can be considered as effective, sustainable, and green environmental catalysts for PET glycolysis reaction [36]. Despite the effective outcomes demonstrated by these calcium oxide catalysts in PET glycolysis reactions, the underlying reaction mechanism remained unclear. This study contemplated the use of DFT calculations [3,37–43] to elucidate the reaction mechanism of PET glycolysis employing a calcium catalyst within the program's research scope. Ca^{2+} was chosen to represent a segment of calcium oxide without environmental factors, while $Ca(OH)_2 \bullet 2H_2O$ was selected to represent a segment of calcium oxide within a congested environment.

Furthermore, poly(etylene furanoate) (PEF) is a bio-based polymer derived from plants. This polymer has the potential to replace the plastic industry's giant poly(ethylene terephthalate) (PET) which is a durable material derived from conventional resources [44,45]. Over the past decade, there has been a growing focus on biobased plastics. This surge of interest is driven by the potential that these materials must diminish anthropogenic greenhouse gas (GHG) emissions and enhance the security of raw material supply. This is achieved through a shift from fossil feedstocks to renewable and sustainably exploited biobased feedstocks [46]. The similarity between these two polymers suggests that the mechanism of polymer degradation may follow a similar pathway. To investigate the role of calcium catalyst in PET and PEF glycolysis reaction, the conformation mechanism of glycolysis reaction, and the possible reaction pathways for the reaction, the degradation of PET and PEF were explored by DFT calculations [47,48].

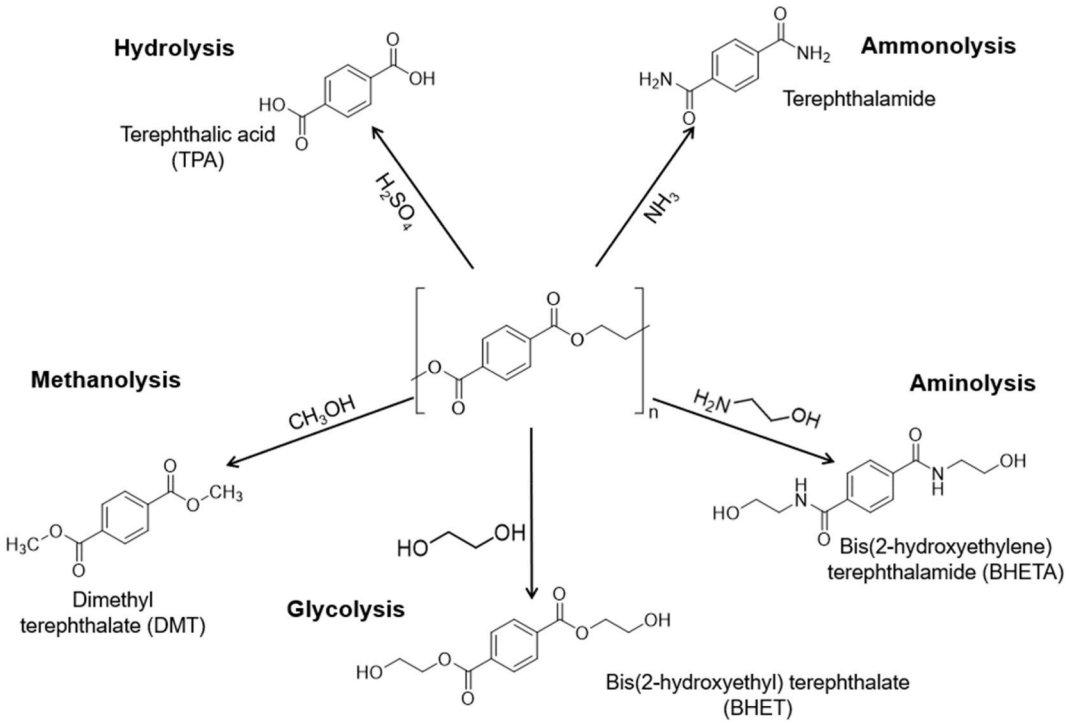

Fig. 1. Chemical recycling methods proposed for depolymerization of PET.

2. Methods

The calculations in this study were carried out by using the Gaussian 16 package [49] at B3LYP/6-31++G(D,P) level for geometry optimization and frequency calculations in gas phase. The same level of theory was used in the transition stage (**TS**) calculations. The stationary points were characterized by frequency calculations to verify that the structures had only one imaginary frequency. Intrinsic reaction coordinate (IRC) [50] calculations were performed to confirm that each transition structure connected to the forward and reverse minima. To study the effect of solvent, the solvation model density method (SMD) [51] was used to perform calculations with the dielectric constant of ethylene glycol (EG) at B3LYP/6-311++G** level to include a dispersion correction term. In this study, 2-hydroxyethyl benzoate and 2-hydroxyethyl furanoate were represented respectively as subunits of PET and PEF. The Cartesian coordinate (XYZ) information of calculated structures was shown in supporting information.

3. Results and discussion

In order to explore the conformation structure of glycolysis reaction of PET, we investigated the mechanism of the C–O cleavage reaction catalyzed by Ca^{2+} and $Ca(OH)_2 \bullet 2H_2O$. The **TS** complexes were calculated and optimized at B3LYP/6-31++G(D,P) level to the reactant by moving hydroxyl hydrogen atom of EG near to hydroxyl oxygen of EG to obtain structure **A**. When **TS** complexes were optimized to the product by moving hydroxyl hydrogen atom of EG to carbonyl ester oxygen of PET, structure **B** can be obtained (Fig. 2a). The calculated energy in gas phase was shown in Table S1 in supporting information. The optimized structure of **A**, **TS**, and **B** at gas phase are shown in Fig. 3. For Ca^{2+}, the **TS** complex formation includes the significant coordination of calcium catalyst with the carbonyl oxygen of the ester group of PET and both of the hydroxyl oxygen of EG. In the absence of ligand coordinating to calcium, both hydroxyl oxygen of EG could coordinate to calcium in **A, TS,** and **B** structures. In contrast, there is only nucleophilic hydroxyl oxygen of EG can coordinate with $Ca(OH)_2 \bullet 2H_2O$ in **A**, **TS**, and **B** structures because of crowded ligands around the calcium center. The glycolysis reaction mechanism was investigated by performing IRC calculation of **TS** structures. In the glycolysis of PET to BHET monomer, both calcium catalysts played the role of cation catalysts and formed coordination with carbonyl oxygen of PET likes Lewis acid including other oxygen atoms in complex that located near the calcium such as, hydroxyl oxygen of PET, and hydroxyl oxygen of EG. Then, one of the protons of hydroxyl oxygen of EG was transferred to the carbonyl oxygen of polymer and the oxygen atom of EG attacked the carbonyl carbon of PET leading to degradation reaction. Therefore, the role of calcium catalysts was mainly forming hydrogen bonds with oxygen of PET. The C–O cleavage proceeded by **TS** with a four-membered ring before degradation including carbonyl carbon of PET (C) and hydroxyl oxygen of EG (O_E), hydroxyl oxygen of EG (O_E) and hydrogen of hydroxyl oxygen of EG (H), hydrogen of hydroxyl oxygen of EG (H) and carbonyl ester oxygen of PET (O_1), and carbonyl ester oxygen of PET (O_1) and carbonyl carbon of PET (C).

After understanding the conformation mechanism of glycolysis reaction using calcium catalysts and complex structures were collected, the solvation model density method (SMD) was used to obtain calculated information in ethylene glycol to reach the information as much as real experimental design. The glycolysis reaction of PET was studied in two different pathways. First, the glycolysis reaction with the coordination of the hydroxyl oxygen of EG to the calcium (Fig. 2a). Second, the hydroxyl oxygen of EG directly attacked the carbonyl carbon of the ester group of PET without the coordination to the calcium (Fig. 2b).

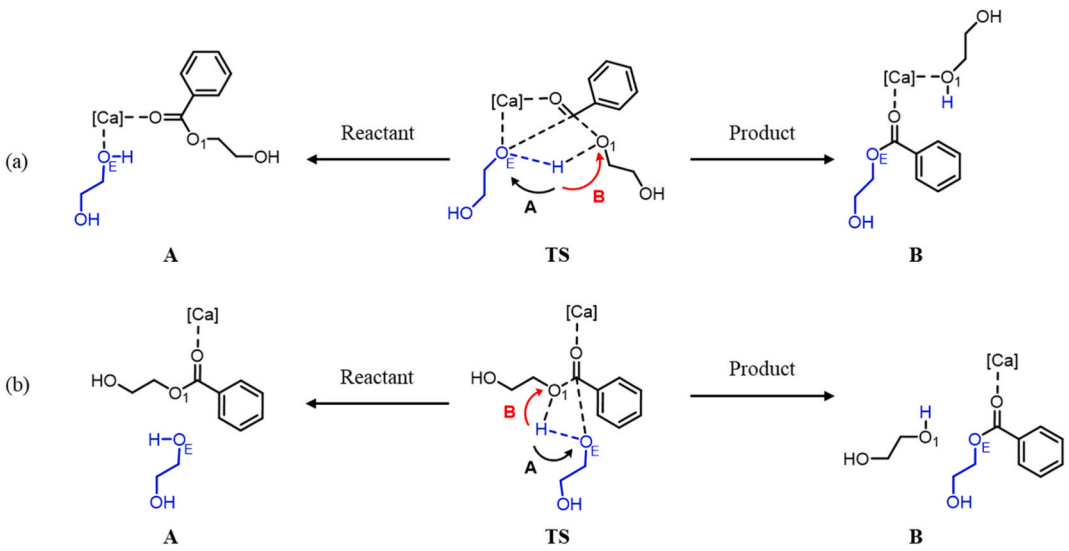

Fig. 2. Structure of **A**, **TS**, and **B** of glycolysis reaction of PET's unit with (a) coordinated EG, (b) non-coordinated EG (O_E = hydroxyl oxygen of EG, H = hydroxyl hydrogen of EG and O_1 = carbonyl ester oxygen).

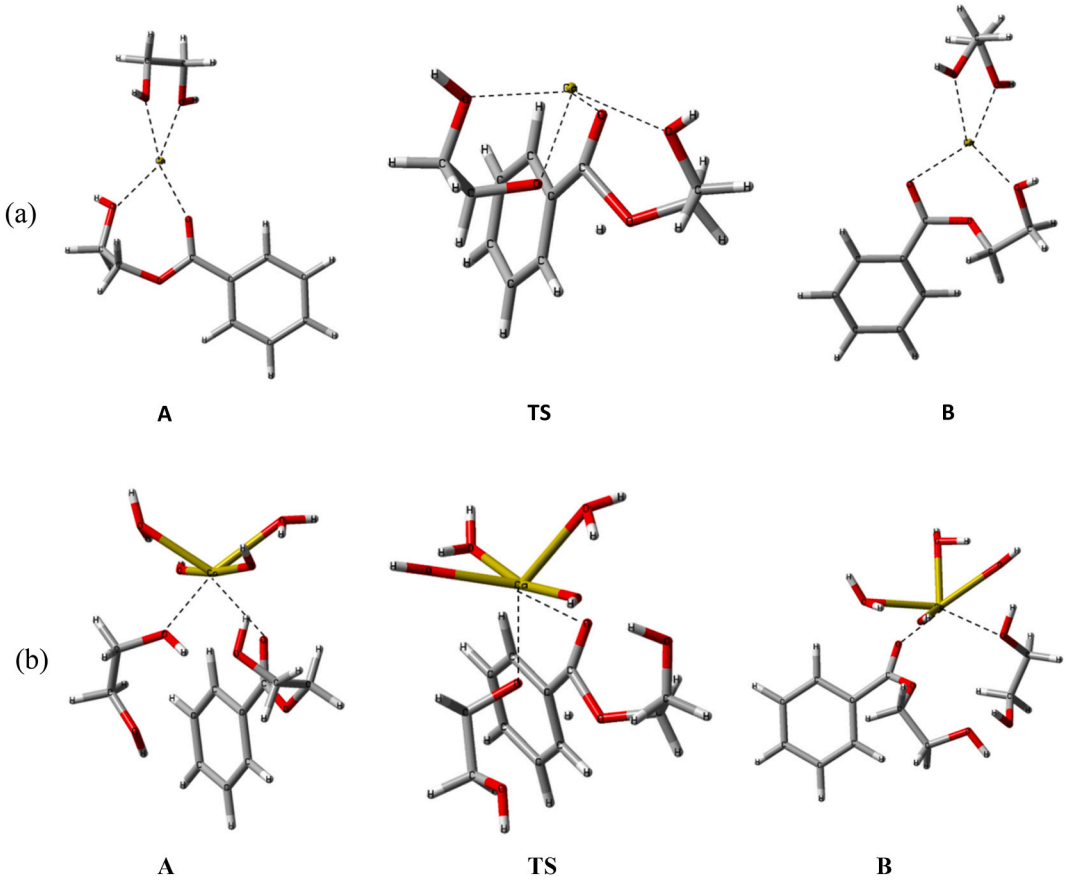

Fig. 3. Optimized structures of **A**, **TS**, and **B** at gas phase for glycolysis of PET catalyzed by: (a) Ca^{2+}, and (b) $Ca(OH)_2 \bullet 2H_2O$.

3.1. The glycolysis reaction with the coordination of the hydroxyl oxygen of EG to the calcium (coordination pathway)

With the SMD correlation, when the Ca^{2+} ion was applied to the reaction, the reaction was induced with the formation of a complex between EG and PET with the calcium ion. When hydrogen atom of EG was located near to the cleavage site in **TS**, the structure was induced to show a bend structure of PET with 96° angle between carbonyl carbon, carbonyl ester oxygen, and hydroxyl oxygen of PET (C−O_E−OH). The hydroxyl oxygen of PET was coordinated with the calcium ion as same as both hydroxyl oxygens of EG (Fig. 4a). The information of four-membered ring of C−O_E, O_E−H, H–O_1, and O_1–C forming can be collected by observation the route of atoms moving to the C–O cleavage site until fragment of degraded PET left in the glycolysis reaction (Tables S2 and S3). The distance between C and O_E of **A1**, **TS1**, and **B1** were 5.55, 1.90, and 1.36 Å respectively whereas the distance between C and O_1 of **A1**, **TS1**, and **B1** were 1.33, 1.63, and 5.30 Å respectively. The energy differences between **TS1** and **A1** (E_A), and **TS1** and **B1** (E_B) were 52.8 and 44.0 kcal mol^{-1} (Fig. 5, Table 1). The structures showed that, without any ligands coordinating to the calcium ion, the distance of C−O_E before the glycolysis reaction was longer than the distance of C–O_1 after the C–O cleavage. The distances between Ca–O_1 of **A1**, and Ca−O_E of **B1** were 4.12, and 2.72 Å respectively (Table S4). The structure showed that, in coordination of hydroxyl oxygen of EG on the calcium, the carbonyl ester oxygen of fragment of PET was closer to the calcium after glycolysis reaction.

The conformational structures of PEF catalyzed by Ca^{2+} were investigated in the same method with the PET. With the Ca^{2+} ion, the hydroxyl oxygen of PEF was coordinated with the calcium ion as same as both hydroxyl oxygen of EG in **TS** (Fig. 6a). The hydroxyl oxygen of PEF bent to the calcium with 87° angle of C−O_E−OH. The distances between C and O_E of **A5**, **TS5**, and **B5** were 5.61, 1.90, and 1.35 Å respectively whereas the distances between C and O_1 of **A5**, **TS5**, and **B5** were 1.33, 1.61, and 5.37 Å respectively. The distance of the C−O_E before the glycolysis reaction was longer than the distance of C–O_1 after the C–O cleavage. The E_A and E_B of the glycolysis reaction were 54.7 and 46.1 kcal mol^{-1}, respectively (Table 2). The distances between Ca–O_1 of **A5**, and Ca−O_E of **B5** were 4.14, and 2.78 Å respectively. The carbonyl ester oxygen of fragment of PEF was closer to the calcium after glycolysis reaction.

However, when $Ca(OH)_2 \bullet 2H_2O$ was applied in the reaction, the complex between EG and PET with the calcium ion showed that EG was located near the PET by the steric effect of crowded ligands at the beginning. Both hydroxyl oxygens of EG coordinated with calcium in **TS**. The complex initiated a bend structure of PET without coordination of hydroxyl oxygen of PET to the calcium due to crowded ligands (Fig. 4b). The hydroxyl oxygen of PET bent to the calcium with 107° angle of C−O_E−OH. The distances between C and O_E of **A2**, **TS2**, and **B2** were 3.37, 1.97, and 1.34 Å respectively while the distances between C and O_1 of **A2**, **TS2**, and **B2** were 1.33,

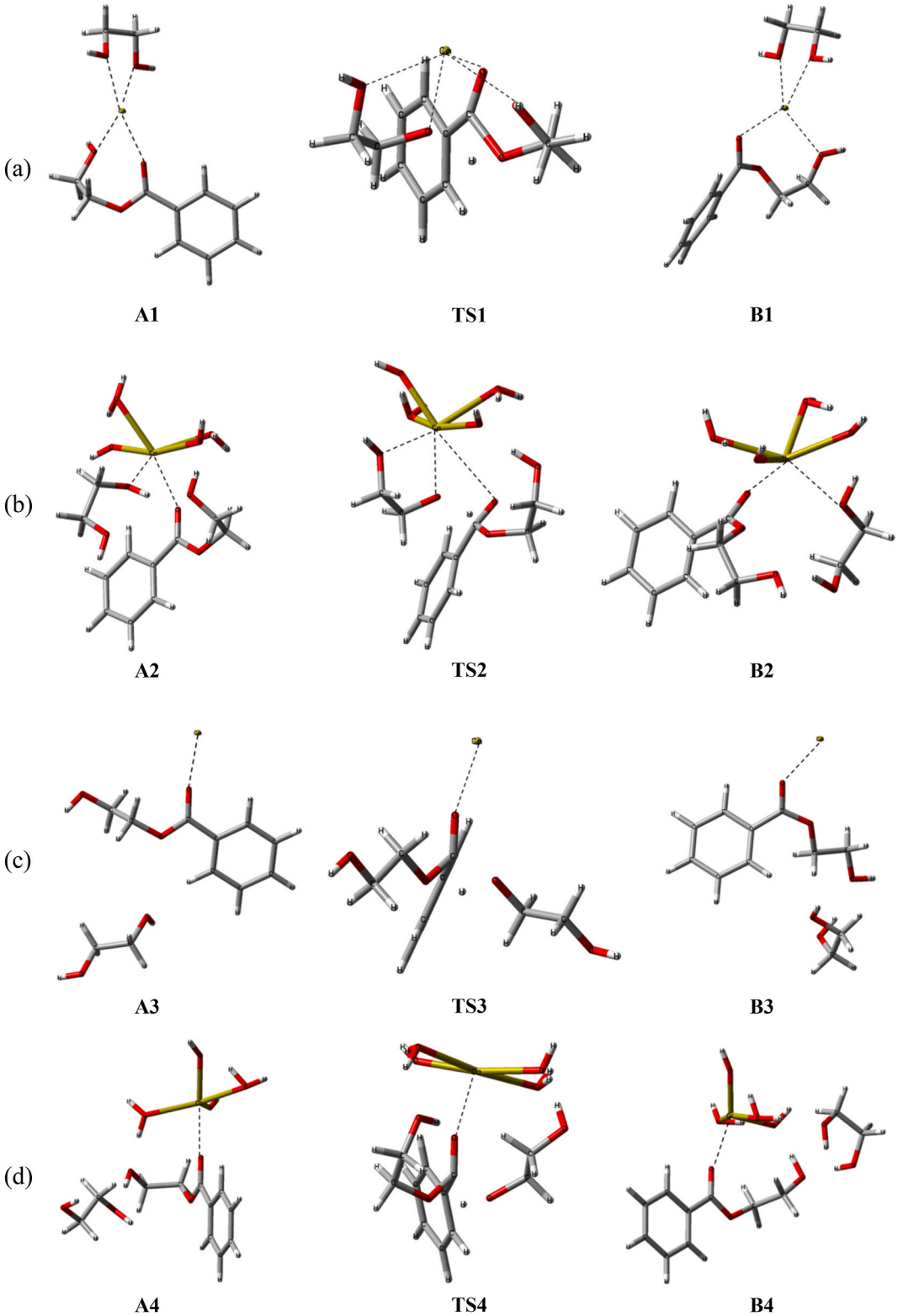

Fig. 4. Optimized structures of **A**, **TS**, and **B** for the glycolysis of PET in ethylene glycol catalyzed by: (a) Ca^{2+} coordination, (b) $Ca(OH)_2 \bullet 2H_2O$ coordination, (c) Ca^{2+} non-coordination, and (d) $Ca(OH)_2 \bullet 2H_2O$ non-coordination.

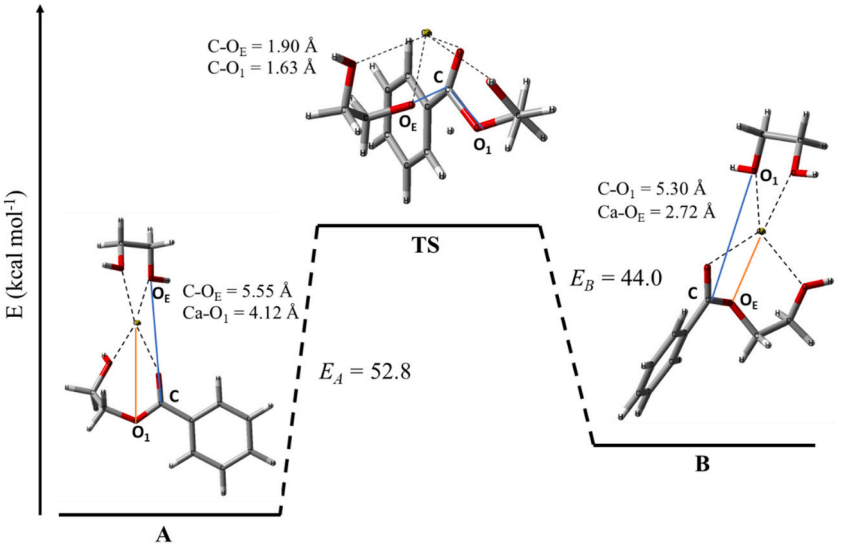

Fig. 5. Relative energy diagram for glycolysis reaction of PET with Ca^{2+} with EG coordination.

Table 1
Calculated lowest energies (kcal mol^{-1}) for the glycolysis of PET catalyzed by calcium catalysts in ethylene glycol at B3LYP/6-311++G** level.

Entry	Catalyst	Coordination		Non-coordination	
		E_A	E_B	E_A	E_B
1	Ca^{2+}	52.8	44.0	49.6	44.8
2	$Ca(OH)_2•2H_2O$	53.6	37.0	52.3	58.0

1.68, and 4.58 Å respectively. The E_A and E_B were 53.6 and 37.0 kcal mol^{-1}, respectively (Table 1). The complexes showed that, the distance of the C−O_E before the glycolysis reaction was shorter than the distance of C–O_1 after the C–O cleavage. In coordination of O_E with the calcium system, EG was forced by crowded ligands of calcium catalyst to be located close to PET. The distances between Ca–O_1 of **A2**, and Ca−O_E of **B2** were 4.40, and 2.81 Å respectively. The carbonyl ester oxygen of fragment of PET is closer to the calcium after glycolysis reaction.

For PEF with $Ca(OH)_2•2H_2O$, both hydroxyl oxygens of EG coordinated with the calcium in **TS**. Hydroxyl oxygen of PEF did not coordinate with the calcium due to crowded ligands (Fig. 6b). The hydroxyl oxygen of PEF bent to the calcium with 107° angle of C−O_E−OH. The distance between C and O_E of **A6**, **TS6**, and **B6** were 4.18, 1.95, and 1.33 Å, respectively while the distance between C and O_1 of **A6**, **TS6**, and **B6** were 1.33, 1.65, and 4.27 Å, respectively. The complexes showed that the distance of the C−O_E before the glycolysis reaction was shorter than the distance of the C–O_1 after the C–O cleavage. The E_A and E_B of the glycolysis reaction were 53.1 and 42.7 kcal mol^{-1}, respectively (Table 2). The distances between Ca–O_1 of **A6**, and Ca−O_E of **B6** were 4.40, and 3.69 Å respectively. The carbonyl ester oxygen of fragment of PEF is closer to the calcium after glycolysis reaction.

For glycolysis of PET and PEF in coordination pathway, the **TS** structure showed that both hydroxyl oxygen of EG coordinated with the calcium catalyst. Without ligands on the calcium, other oxygens such as hydroxyl oxygen on subunit of the polymer possibly coordinated with the catalyst. Besides, according to free space around the calcium ion, Ca^{2+} had more distances for atoms shifting to reach four-membered C–O cleavage site than $Ca(OH)_2•2H_2O$. The carbonyl ester oxygen of the fragment polymer after glycolysis was located near to the calcium because it belonged to coordinated hydroxyl oxygen of EG before C–O cleavage.

3.2. The glycolysis reaction without the coordination of the hydroxyl oxygen of EG to the calcium (non-coordination pathway)

Considering the pathway that hydroxyl oxygen of EG would attack on the carbonyl carbon of the polymer directly without the coordination of hydroxyl oxygen of EG with the calcium. When Ca^{2+} was applied to the glycolysis reaction of PET, the reaction was induced with coordination between carbonyl oxygen of PET and the calcium ion. The EG was located near the PET without any coordination of O_E to the calcium ion. When a hydroxyl hydrogen atom of EG was transferred near to the cleavage site, the complex set to a bend structure of PET without coordination of O_E with the calcium ion (Fig. 4c). The hydroxyl oxygen of PET did not bend to calcium ion with angle of C−O_E−OH was 139°. The distances between C and O_E of **A3**, **TS3**, and **B3** were 4.80, 1.67, and 1.33 Å respectively whereas the distances between C and O_1 of **A3**, **TS3**, and **B3** were 1.33, 1.62, and 5.70 Å respectively. The E_A and E_B of the glycolysis reaction were 49.6 and 44.8 kcal mol^{-1} (Table 1). The distance of the C−O_E before the glycolysis reaction was shorter than the distance of the C–O_1 after the C–O cleavage. The distances between Ca–O_1 of **A3**, and Ca−O_E of **B3** were 4.54, and 3.69 Å respectively. The

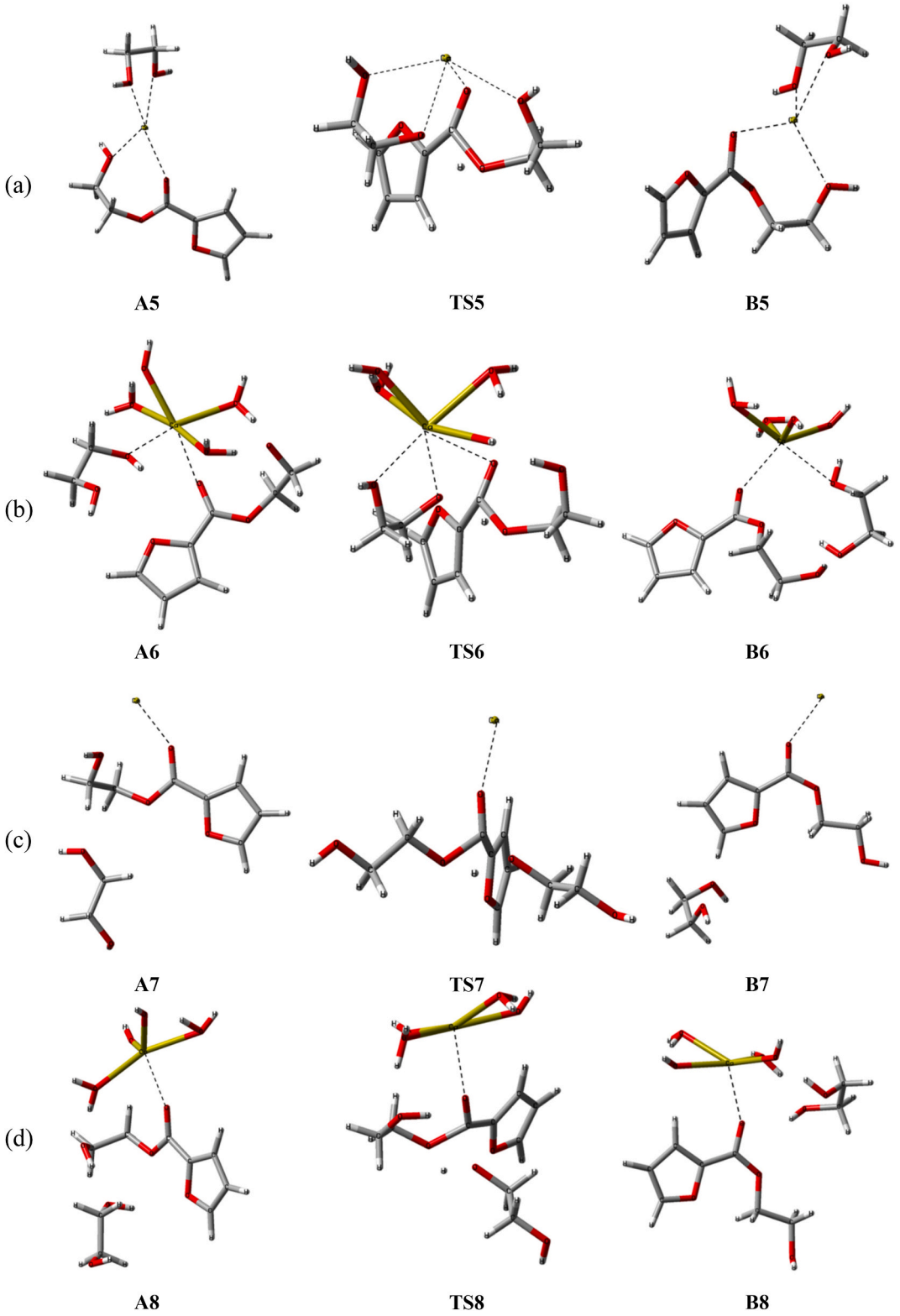

Fig. 6. Optimized structures of **A**, **TS**, and **B** for glycolysis of PEF in ethylene glycol catalyzed by: (a) Ca^{2+} coordination, (b) $Ca(OH)_2 \bullet 2H_2O$ coordination, (c) Ca^{2+} non-coordination, and (d) $Ca(OH)_2 \bullet 2H_2O$ non-coordination.

Table 2
Calculated lowest energies (kcal mol^{-1}) for the glycolysis of PEF catalyzed by calcium catalysts in ethylene glycol at B3LYP/6-311++G** level.

Entry	Catalyst	Coordination		Non-coordination	
		E_A	E_B	E_A	E_B
1	Ca^{2+}	54.7	46.1	55.2	46.9
2	$Ca(OH)_2•2H_2O$	53.1	42.7	57.0	56.8

carbonyl ester oxygen of fragment of PET is closer to the calcium after glycolysis reaction. Although O_E was not coordinated with the calcium ion before the reaction, O_E that became carbonyl ester oxygen instead of O_1 after the glycolysis was affected by cation of the calcium. The structure adapted to a bend structure with carbonyl ester oxygen of fragment of PET close to the calcium.

For PEF with Ca^{2+} in non-coordination pathway (Fig. 6c), the hydroxyl oxygen of PEF did not bend to calcium ion with angle of C−O_E−OH was 138°. The distance between C and O_E of **A7**, **TS7**, and **B7** were 5.24, 1.64, and 1.33 Å respectively whereas the distance between C and O_1 of **A7**, **TS7**, and **B7** were 1.33, 1.62, and 6.56 Å respectively. In non-coordination system, the distance of the C−O_E before the glycolysis reaction was shorter than the distance of the C–O_1 after the C–O cleavage. The E_A and E_B of the glycolysis reaction were 55.2 and 46.9 kcal mol^{-1}, respectively (Table 2). The distances between Ca–O_1 of **A7**, and Ca−O_E of **B7** were 4.09, and 3.84 Å. The carbonyl ester oxygen of fragment of PEF is also closer to the calcium after glycolysis reaction in the same way with PET.

However, when $Ca(OH)_2•2H_2O$ was applied, the EG was located near PET without the steric effect of crowded ligands of the calcium. When a hydroxyl hydrogen atom of EG was transferred near to the cleavage site, the complex initiated a bend structure of PET without coordination of O_E with the calcium (Fig. 4d). The hydroxyl oxygen of PET bent to the calcium with 86° angle of C−O_E−OH. The distances between C and O_E of **A4**, **TS4**, and **B4** were 4.02, 1.58, and 1.33 Å respectively while the distances between C and O_1 of **A4**, **TS4**, and **B4** were 1.33, 1.62, and 6.34 Å respectively. The E_A and E_B of the glycolysis reaction were 52.3 and 58.0 kcal mol^{-1} (Table 1). The distance of the C−O_E before the glycolysis reaction was shorter than the distance of the C–O_1 after the C–O cleavage. The distances between Ca–O_1 of **A4**, and Ca−O_E of **B4** were 4.40, and 4.36 Å respectively. Without coordination of O_E to $Ca(OH)_2•2H_2O$, after the glycolysis, the cation had a small effect on the carbonyl ester oxygen of fragment of PET because of crowded ligands.

The same phenomena could be observed in glycolysis reaction of PEF with $Ca(OH)_2•2H_2O$ in non-coordination pathway (Fig. 6d). The hydroxyl oxygen of PEF bent to the calcium with 82° angle of C−O_E−OH. The distances between C and O_E of **A8**, **TS8**, and **B8** were 3.69, 1.65, and 1.33 Å, respectively while the distance between C and O_1 of **A8**, **TS8**, and **B8** were 1.33, 1.60, and 4.48 Å, respectively. The distance of C−O_E before the glycolysis reaction was shorter than the distance of C–O_1 after the C–O cleavage. The E_A and E_B of glycolysis reaction were 57.0 and 56.8 kcal mol^{-1}, respectively (Table 2). The distances between Ca–O_1 of **A8**, and Ca−O_E of **B8** were 4.40, and 4.65 Å. Without coordination of O_E to the calcium, after the glycolysis, O_E that became carbonyl ester oxygen instead of O_1 was located far from the calcium.

In the non-coordination pathway, the calcium catalyst mainly coordinated with the carbonyl oxygen atoms of PET and PEF. Without any ligand on the calcium, the **TS** complexes formation was promoted to be symmetric. When **TS** structures were optimized to **A**, there was no critical different distance between O_E and C for both Ca^{2+} and $Ca(OH)_2•2H_2O$. EG was located near to the carbonyl carbon of the subunit of the polymer before glycolysis reaction. On the other hand, when the **TS** was optimized to **B**, the left part of the fragment degraded polymers was settled far away after breaking the four-membered ring complex. The carbonyl ester oxygen of the fragment polymer was located close to the Ca^{2+}, even if the calcium ion was not coordinated by EG due to the cationic effect. In contrast to $Ca(OH)_2•2H_2O$, the crowded ligands causing steric environment around the calcium. The carbonyl ester oxygen of the fragment polymer also got small effect from cation catalyst and did not locate significantly close to $Ca(OH)_2•2H_2O$.

Based on our DFT calculations, the glycolysis reaction of PET in the non-coordination pathway seemed to have smaller E_A compared to the coordination pathway. In addition, the reaction with Ca^{2+} also had smaller E_A than $Ca(OH)_2•2H_2O$ around 0.8 kcal mol^{-1} for the coordination pathway and 2.7 kcal mol^{-1} for the non-coordination pathway. It was found that free space around the catalyst enhanced the glycolysis reaction of PET. As a result, the Ca−based catalyst that suitable for PET glycolysis reaction should occupy free area around the active site. No matter that ethylene glycol would coordinate with the catalyst or not, the reaction would be more favorable with free calcium catalyst than the calcium with ligands. On the other hand, the glycolysis reaction of PEF in the coordination pathway had smaller E_A than the non-coordination pathway. For the coordination pathway, the E_A of the $Ca(OH)_2•2H_2O$ showed 1.6 kcal mol^{-1} lower than the one of Ca^{2+} while the E_A of the $Ca(OH)_2•2H_2O$ showed 1.8 kcal mol^{-1} higher than the one of Ca^{2+} for the non-coordination pathway. Without the coordination of ethylene glycol on the calcium catalyst before the glycolysis reaction, the environment around the catalyst had a small effect on the direction of ethylene glycol attacking PEF.

4. Conclusion

In summary, conformational mechanisms of PET and PEF glycolysis reactions with calcium catalysts can be predicted through the transition complex investigation by DFT calculations. To account for the effect of solvent, the solvation model density (SMD) was applied to the calculations. The SMD correlation influenced the structure formation indicated the different conformation structures between gas phase and solvent phase calculations. The degradation of PET and PEF *via* glycolysis reactions followed steps by calcium catalysts coordinated with the carbonyl oxygen of polymer. Then, the hydrogen atom transfers from the hydroxyl of EG to the ester oxygen of the polymer and the hydroxyl oxygen attacks the carbonyl carbon of the polymer initiating the C–O cleavage to form a monomer unit. The conformation mechanism of four-centered cleavage site can be observed by intrinsic reaction coordinate (IRC)

calculation. The calcium catalysts, Ca^{2+} and $Ca(OH)_2 \bullet 2H_2O$, represented the different environment around the active site of the catalyst caused various conformation structures that affected the energy barrier for glycolysis reactions. Two different pathways, the coordination and non-coordination of EG with calcium, also provided different conformation structures and energy barrier for glycolysis reactions. This study proposed the conformation mechanisms of the glycolysis reaction involving PET and PEF, offering insights for catalysts choosing and for the future design of exceptionally efficient calcium catalysts for the reaction.

Data availability statement

The data that support the findings of this study are available on request from the corresponding author.

CRediT authorship contribution statement

Anyarin Arunphacharawit: Writing – original draft, Visualization, Validation, Methodology, Formal analysis. **Thinnaphat Poonsawat:** Writing – review & editing. **Titiya Meechai:** Writing – review & editing, Conceptualization. **Laksamee Chaicharoenwimolkul Chuaitammakit:** Writing – review & editing, Conceptualization. **Ekasith Somsook:** Writing – original draft, Supervision, Project administration, Methodology, Investigation, Conceptualization.

Declaration of competing interest

The authors declare the following financial interests/personal relationships which may be considered as potential competing interests: Ekasith Somsook reports financial support was provided by Mahidol University. If there are other authors, they declare that they have no known competing financial interests or personal relationships that could have appeared to influence the work reported in this paper.

Acknowledgements

This work is funded by National Research Council of Thailand (NRCT) and Mahidol University [Grant No. N42A650355], the NSRF *via* the Program Management Unit for Human Resources & Institutional Development, Research, and Innovation [Grant No. B16F640099] and a research grant from theCenter of Excellence for Innovation in Chemistry (PERCH-CIC).

Appendix A. Supplementary data

Supplementary data to this article can be found online at https://doi.org/10.1016/j.heliyon.2024.e34666.

References

[1] R.C. Thompson, Y. Olsen, R.P. Mitchell, A. Davis, S.J. Rowland, A.W. John, D. McGonigle, A.E. Russell, Lost at sea: where is all the plastic? Science 304 (2004) 838, 838.
[2] T. Romeo, B. Pietro, C. Pedà, P. Consoli, F. Andaloro, M.C. Fossi, First evidence of presence of plastic debris in stomach of large pelagic fish in the Mediterranean Sea, Mar. Pollut. Bull. 95 (2015) 358–361.
[3] D.M. Teegarden, Polymer Chemistry, introduction to an indispensable science (NSTA Press), 2004.
[4] E. Lokensgard, Industrial Plastics, theory and applications (Cengage Learning), 2016.
[5] V. Sinha, M.R. Patel, J.V. Patel, PET waste management by chemical recycling: a review, J. Polym. Environ. 18 (2010) 8–25.
[6] J.R. Jambeck, R. Geyer, C. Wilcox, T.R. Siegler, M. Perryman, A. Andrady, R. Narayan, K.L. Law, Plastic waste inputs from land into the ocean, Science 347 (2015) 768–771.
[7] R. Geyer, J.R. Jambeck, K.L. Law, Production, use, and fate of all plastics ever made, Sci. Adv. 3 (2017) 1700782, e.
[8] M. Chanda, S.K. Roy, Plastics Fabrication and Recycling (CRC Press), 2016.
[9] A. Al-Sabagh, F. Yehia, D.R. Harding, G. Eshaq, A. ElMetwally, Fe 3 O 4-boosted MWCNT as an efficient sustainable catalyst for PET glycolysis, Green Chem. 18 (2016) 3997–4003.
[10] G. Giannotta, R. Po, N. Cardi, E. Tampellini, E. Occhiello, F. Garbassi, L. Nicolais, Processing effects on poly (ethylene terephthalate) from bottle scraps, Polym. Eng. Sci. 34 (1994) 1219–1223.
[11] M. Genta, T. Iwaya, M. Sasaki, M. Goto, T. Hirose, Depolymerization mechanism of poly (ethylene terephthalate) in supercritical methanol, Ind. Eng. Chem. Res. 44 (2005) 3894–3900.
[12] M.J. Collins, S.H. Zeronian, M.L. Marshall, Analysis of the molecular weight distributions of aminolyzed poly (ethylene terephthalate) by using gel permeation chromatography, J. Macromol. Sci.-Chem. 28 (1991) 775–792.
[13] M. Khoonkari, A.H. Haghighi, Y. Sefidbakht, K. Shekoohi, A. Ghaderian, Chemical recycling of PET wastes with different catalysts, Int. J. Polym. Sci. 2015 (2015).
[14] L. Bartolome, M. Imran, B.G. Cho, W.A. Al-Masry, D.H. Kim, Recent developments in the chemical recycling of PET, Mater. Recycl.-Trend. Perspect. 406 (2012) 576–596.
[15] G. Xi, M. Lu, C. Sun, Study on depolymerization of waste polyethylene terephthalate into monomer of bis (2-hydroxyethyl terephthalate), Polym. Degrad. Stabil. 87 (2005) 117–120.
[16] M. Ghaemy, K. Mossaddegh, Depolymerisation of poly (ethylene terephthalate) fibre wastes using ethylene glycol, Polym. Degrad. Stabil. 90 (2005) 570–576.
[17] N.D. Pingale, V.S. Palekar, S. Shukla, Glycolysis of postconsumer polyethylene terephthalate waste, J. Appl. Polym. Sci. 115 (2010) 249–254.
[18] S. Shukla, A.M. Harad, Glycolysis of polyethylene terephthalate waste fibers, J. Appl. Polym. Sci. 97 (2005) 513–517.

[19] M.M.A. Nikje, F. Nazari, Microwave-assisted depolymerization of poly (ethylene terephthalate)[PET] at atmospheric pressure, Adv. Polym. Technol.: J. Polym. Proc. Inst. 25 (2006) 242–246.
[20] K. Troev, G. Grancharov, R. Tsevi, I. Gitsov, A novel catalyst for the glycolysis of poly (ethylene terephthalate), J. Appl. Polym. Sci. 90 (2003) 1148–1152.
[21] I. Duque-Ingunza, R. López-Fonseca, B. De Rivas, J. Gutiérrez-Ortiz, Synthesis of unsaturated polyester resin from glycolysed postconsumer PET wastes, J. Mater. Cycles Waste Manag. 15 (2013) 256–263.
[22] S. Shukla, K. Kulkarni, Depolymerization of poly (ethylene terephthalate) waste, J. Appl. Polym. Sci. 85 (2002) 1765–1770.
[23] T. Christoff-Tempesta, T.H. Epps III, Ionic-liquid-mediated deconstruction of polymers for advanced recycling and upcycling, ACS Macro Lett. 12 (2023) 1058–1070.
[24] K.S. Egorova, V.P. Ananikov, Toxicity of ionic liquids: eco (cyto) activity as complicated, but unavoidable parameter for task-specific optimization, ChemSusChem 7 (2014) 336–360.
[25] C.-W. Cho, T.P.T. Pham, Y. Zhao, S. Stolte, Y.-S. Yun, Review of the toxic effects of ionic liquids, Sci. Total Environ. 786 (2021) 147309.
[26] T.P.T. Pham, C.-W. Cho, Y.-S. Yun, Environmental fate and toxicity of ionic liquids: a review, Water Res. 44 (2010) 352–372.
[27] A.R. Gonçalves, X. Paredes, A. Cristino, F. Santos, C.S. Queirós, Ionic liquids—a review of their toxicity to living organisms, Int. J. Mol. Sci. 22 (2021) 5612.
[28] A. Al-Sabagh, F. Yehia, A. Eissa, M. Moustafa, G. Eshaq, A. Rabie, A. ElMetwally, Cu-and Zn-acetate-containing ionic liquids as catalysts for the glycolysis of poly (ethylene terephthalate), Polym. Degrad. Stabil. 110 (2014) 364–377.
[29] M. Imran, K.G. Lee, Q. Imtiaz, B.-k. Kim, M. Han, B.G. Cho, D.H. Kim, Metal-oxide-doped silica nanoparticles for the catalytic glycolysis of polyethylene terephthalate, J. Nanosci. Nanotechnol. 11 (2011) 824–828.
[30] M. Imran, W.A. Al-Masry, A. Mahmood, A. Hassan, S. Haider, S.M. Ramay, Manganese-, cobalt-, and zinc-based mixed-oxide spinels as novel catalysts for the chemical recycling of poly (ethylene terephthalate) via glycolysis, Polym. Degrad. Stabil. 98 (2013) 904–915.
[31] R. López-Fonseca, I. Duque-Ingunza, B. De Rivas, S. Arnaiz, J.I. Gutierrez-Ortiz, Chemical recycling of post-consumer PET wastes by glycolysis in the presence of metal salts, Polym. Degrad. Stabil. 95 (2010) 1022–1028.
[32] H. Wang, Y. Liu, Z. Li, X. Zhang, S. Zhang, Y. Zhang, Glycolysis of poly (ethylene terephthalate) catalyzed by ionic liquids, Eur. Polym. J. 45 (2009) 1535–1544.
[33] K.H. Zangana, A. Fernandez, J.D. Holmes, Simplified, fast, and efficient microwave assisted chemical recycling of poly (ethylene terephthalate) waste, Mater. Today Commun. 33 (2022) 104588.
[34] G. Park, L. Bartolome, K.G. Lee, S.J. Lee, T.J. Park, One-step sonochemical synthesis of a graphene oxide–manganese oxide nanocomposite for catalytic glycolysis of poly (ethylene terephthalate), Nanoscale 4 (2012) 3879–3885.
[35] L. Bartolome, M. Imran, K.G. Lee, A. Sangalang, J.K. Ahn, Superparamagnetic γ-Fe 2 O 3 nanoparticles as an easily recoverable catalyst for the chemical recycling of PET, Green Chem. 16 (2014) 279–286.
[36] I. Yunita, S. Putisompon, P. Chumkaeo, T. Poonsawat, E. Somsook, Effective catalysts derived from waste ostrich eggshells for glycolysis of post-consumer PET bottles, Chem. Pap. 73 (2019) 1547–1560.
[37] Z. Ju, L. Zhou, X. Lu, Y. Li, X. Yao, S. Cheng, G. Chen, C. Ge, Mechanistic insight into the roles of anions and cations in the degradation of poly (ethylene terephthalate) catalyzed by ionic liquids, Phys. Chem. Chem. Phys. 23 (2021) 18659–18668.
[38] P. Hohenberg, W. Kohn, Structural properties of copper, Phys. Rev. 136 (1964) B864–B871.
[39] W. Kohn, L. Sham, Self-consistent equations including exchange and correlation effects, Phys. Rev. 140 (1965) a1133–a1138.
[40] R. Arulraj, S. Sivakumar, S. Suresh, K. Anitha, Synthesis, vibrational spectra, DFT calculations, Hirshfeld surface analysis and molecular docking study of 3-chloro-3-methyl-2, 6-diphenylpiperidin-4-one, Spectrochim. Acta Mol. Biomol. Spectrosc. 232 (2020) 118166.
[41] R. Arulraj, S. Sivakumar, K. Rajkumar, J.P. Jasinski, M. Kaur, A. Thiruvalluvar, Synthesis, crystal structure, DFT calculations and hirshfeld surface analysis of 3-Chloro-3-methyl-r (2), c (6)-bis (p-methoxyphenyl) piperidin-4-one, J. Chem. Crystallogr. 50 (2020) 41–51.
[42] A. Ramalingam, S. Kansız, N. Dege, S. Sambandam, Synthesis, crystal structure, DFT calculations and Hirshfeld surface analysis of 3-chloro-2, 6-bis (4-chlorophenyl)-3-methylpiperidin-4-one, J. Chem. Crystallogr. 51 (2021) 273–287.
[43] A. Ramalingam, S. Sambandam, M. Medimagh, O. Al-Dossary, N. Issaoui, M.J. Wojcik, Study of a New Piperidone as an Anti-alzheimer Agent: Molecular Docking, Electronic and Intermolecular Interaction Investigations by DFT Method, Journal of King Saud University-Science 33, 2021, p. 101632.
[44] C.M. Mendieta, G. González, M.E. Vallejos, M.C. Area, Bio-polyethylene furanoate (Bio-PEF) from lignocellulosic biomass adapted to the circular bioeconomy, Bioresources 17 (2022) 7313–7337, https://doi.org/10.15376/biores.17.4.Mendieta.
[45] A.J.J.E. Eerhart, W.J.J. Huijgen, R.J.H. Grisel, J.C. van der Waal, E. de Jong, A. de Sousa Dias, A.P.C. Faaij, M.K. Patel, Fuels and plastics from lignocellulosic biomass via the furan pathway; a technical analysis, RSC Adv. 4 (2014) 3536–3549, https://doi.org/10.1039/c3ra43512a.
[46] A. Eerhart, A. Faaij, M. Patel, Replacing fossil based PET with biobased PEF; process analysis, energy and GHG balance, Energy Environ. Sci. 5 (2012) 6407–6422.
[47] K. Dong, Y. Song, X. Liu, W. Cheng, X. Yao, S. Zhang, Understanding structures and hydrogen bonds of ionic liquids at the electronic level, J. Phys. Chem. B 116 (2012) 1007–1017.
[48] Z. Ju, W. Xiao, X. Lu, X. Liu, X. Yao, X. Zhang, S. Zhang, Theoretical studies on glycolysis of poly (ethylene terephthalate) in ionic liquids, RSC Adv. 8 (2018) 8209–8219.
[49] M. Frisch, G. Trucks, H. Schlegel, G. Scuseria, M. Robb, J. Cheeseman, G. Scalmani, V. Barone, G. Petersson, H. Nakatsuji, G. Aussian 16, Revision A. 03, Gaussian. Inc, Wallingford CT 3, 2016.
[50] C. Gonzalez, H.B. Schlegel, Improved algorithms for reaction path following: higher-order implicit algorithms, J. Chem. Phys. 95 (1991) 5853–5860.
[51] A.V. Marenich, C.J. Cramer, D.G. Truhlar, Universal solvation model based on solute electron density and on a continuum model of the solvent defined by the bulk dielectric constant and atomic surface tensions, J. Phys. Chem. B 113 (2009) 6378–6396.